ACS Macro Letters

Letter

pubs.acs.org/macroletters

Functional Group Distribution and Gradient Structure Resulting from the Living Anionic Copolymerization of Styrene and *para*-But-3-enyl Styrene

Adrian Natalello,[†,‡] Arda Alkan,[†,§] Philipp von Tiedemann,[†] Frederik R. Wurm,*[,§] and Holger Frey*[,†]

[†]Institute of Organic Chemistry, Johannes Gutenberg-University (JGU), Duesbergweg 10-14, 55128 Mainz, Germany

[‡]Graduate School Materials Science in Mainz, Staudinger Weg 9, D-55128 Mainz, Germany

[§]Max Planck Institute for Polymer Research (MPI-P), Ackermannweg 10, D-55128 Mainz, Germany

Supporting Information

ABSTRACT: The functional group distribution along the polymer backbone resulting from the living anionic copolymerization of styrene (S) and *para*-but-3-enyl styrene (*p*BuS) was investigated in cyclohexane at room temperature. A variety of copolymers with different comonomer contents $x(S) = 0-0.84$ have been synthesized with molecular weight dispersities $M_w/M_n \leq 1.12$. All polymers have been characterized in detail by ^{1}H NMR spectroscopy, size exclusion chromatography (SEC), and differential scanning calorimetry (DSC). A detailed understanding of the monomer sequence distribution during the copolymerization was achieved by real-time ^{1}H NMR spectroscopy. This technique permits us to determine the changing monomer concentration of each monomer in stock throughout the reaction. Consequently, monomer incorporation and thus the probability of incorporation can be determined at any time of the copolymerization, and a precise determination of the functional group density along the polymer chain is possible. To demonstrate accessibility of the olefin side chains of the copolymer for transformations, quantitative thiol−ene addition of a cysteine derivative has been studied.

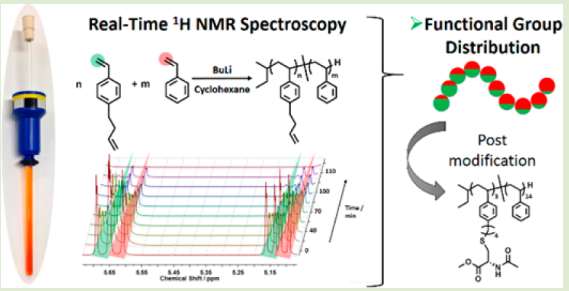

Living anionic polymerization (LAP) was discovered 60 years ago by Michael Szwarc and still represents the key technique in terms of high molecular weight (MW) polymers, narrow molecular weight distributions (MWDs), block copolymers, terminal functionalized polymers, and complex polymer architectures.[1−7] Even if functional groups are limited in carbanionic polymerizations, the control of MW without the use of a heavy metal catalyst or additional ligands makes this technique superior to many other controlled polymerization techniques. However, in contrast to radical polymerization, simultaneous copolymerization (often called "random copolymerization") of different monomers by living (carb)anionic polymerization is a rather neglected field, although a detailed understanding and control of the monomer sequence distribution during a copolymerization are of growing interest.[8−11] First attempts to tailor the monomer sequence distribution in LAP were made 50 years ago. For example, knowing that diphenylethylene (DPE) does not self-propagate, Okamoto and co-workers synthesized alternating copolymers of DPE with styrene (S), isoprene (I), or butadiene.[12−14] Recently, Hutchings and co-workers enlarged this concept investigating the simultaneous terpolymerization of S, DPE, and functionalized DPE derivatives. Due to different electron densities of the double bonds in pure DPE and the functionalized analogues, an enhanced degree of monomer sequence control has been achieved.[15,16]

In contrast, direct oxyanionic copolymerizations of epoxide derivatives which are usually more tolerant to impurities but, above all, much slower have been investigated in several reports. Relying on the rather slow propagation of living oxyanionic copolymerizations our group investigated the monomer sequence distribution during the polymerization via real-time ^{1}H NMR or ^{13}C NMR spectroscopy.[17,18] This technique allows us to follow the consumption of each monomer, respectively, and the growth of the polymer backbone at any point of the polymerization.[19−21] Very recently, we studied carbanionic copolymerizations by real-time ^{1}H NMR spectroscopy of two different comonomer pairs: Although the vinyl bonds of the protected *p*-hydroxystyrene (*p*HS) derivatives, *p*-(1-ethoxy ethoxy)styrene (*p*EES) and 4-*tert*-butoxystyrene (*t*BuOS), appear to be chemically very similar, it was found that *t*BuOS was incorporated preferentially. As expected, the copolymerization of the chemically more different comonomers S and *p*EES leads to a pronounced gradient polymer structure.[22]

Surprisingly, to date only very few reports use in situ techniques to follow living copolymerizations.[23−25] In 1993 Long and co-workers investigated the copolymerization of S

Received: April 28, 2014
Accepted: May 27, 2014
Published: May 30, 2014

and I by near-infrared spectroscopy.[26] Fontanille, Gnanou et al. further expanded this work by combining mid-infrared and UV−visible spectroscopy.[27]

In 1999 Ruckenstein introduced the nonprotected bifunctional monomer 4-(vinylphenyl)-1-butene and investigated the living anionic homo- and copolymerization with S.[28,29] We prefer to handle this compound as *para*-but-3-enyl styrene (*p*BuS) to clarify the relation to S. This monomer is interesting as it allows the direct introduction of olefins via carbanionic polymerization (without protective groups). A different reactivity of *p*BuS and S is expected due to the inductive effects of the substituent. Herein, we use the real-time ^{1}H NMR spectrometric tool to investigate the living anionic copolymerization behavior of S with *p*BuS in cyclohexane at room temperature. To the best of our knowledge this is the first report on the sequence distribution monitoring of a copolymerization via real-time ^{1}H NMR spectroscopy using a nonprotected bifunctional comonomer. Monomer sequence distribution is the key for many applications and to mimic control of biological molecules. Achieving this knowledge is of high importance and would be desirable to gain with classical monomers and polymerization techniques.

We chose *p*BuS as a bifunctional monomer that is suitable for carbanionic polymerization and reinvestigate the copolymerization with S with respect to monomer sequence distribution.[28,29] To monitor the monomer sequence in situ, we first investigated the homopolymerization of *p*BuS in cyclohexane to restrict the reaction kinetics. From the data shown in the Supporting Information (SI) (Table S1 and Figure S2 SEC), it is obvious that prolonged reaction times lead to bimodal MWDs due to branching side reactions with the pendant double bonds. However, for reaction times not exceeding 2.5 h, narrow and monomodal molecular weight distributions are obtained, and no side reactions are observed in the ^{13}C NMR spectrum (Figure S3, SI). However, to guarantee quantitative monomer conversion, no polymers with molecular weights higher than 6700 g·mol^{-1} have been synthesized (see Table 1). Well-defined copolymers with high MW are accessible only in polar solvent mixtures (of toluene and THF (2:1 by volume) at −40 °C) resulting in strongly reduced reaction times which are undesirable for the in situ kinetics studied herein.[29] All synthesized polymers have been characterized by SEC, ^{1}H NMR spectroscopy, and differential scanning calorimetry (DSC).

Table 1. Characterization Data for Homo- and Copolymers Based on *para*-But-3-enyl Styrene (*p*BuS) and Styrene (S)

#	polymer[a]	x(S)[b]	M_n[a]	M_n[c]	$Đ$[c]	T_g/°C[d]
1	P*p*BuS$_{42}$	0	6700	7900	1.12	−13
2	P*p*BuS$_{33}$-*co*-PS$_{6.5}$	0.18	6000	6600	1.11	22
3	P*p*BuS$_{14}$-*co*-PS$_{14}$	0.50	3700	4500	1.12	35
4	P*p*BuS$_3$-*co*-PS$_{14}$	0.79	2000	2100	1.09	40
5	P*p*BuS$_4$-*co*-PS$_{33}$	0.90	4100	4100	1.08	45
6	(P*p*BuS-Cys)$_3$-*co*-PS$_{14}$	0.79	2500	2500	1.10	n.d.

[a]Number-average molecular weight (in g·mol^{-1}), calculated from ^{1}H NMR spectra. [b]Mole fraction styrene. [c]Number-average molecular weight and molecular weight dispersity $Đ$ determined via SEC in DMF (vs PS standards). [d]Glass transition temperature (T_g) determined via DSC.

In contrast to PS (M_n = 4000 g·mol^{-1}) with a glass transition temperature (T_g) of ca. 80 °C,[30] P*p*BuS (#1, M_n = 6 700 g·mol^{-1}) exhibits a rather low T_g of −13 °C, which is clearly a consequence of the flexible butenyl side chains. With increasing amount of S within the copolymers, P*p*BuS-*co*-PS (#2−5, at similar molecular weight), the T_g values also increase, reflecting the (co)polymer composition (Scheme 1).

Scheme 1. Synthetic Strategy for the Synthesis of P*p*BuS-*co*-PS and Subsequent Cysteine Functionalization

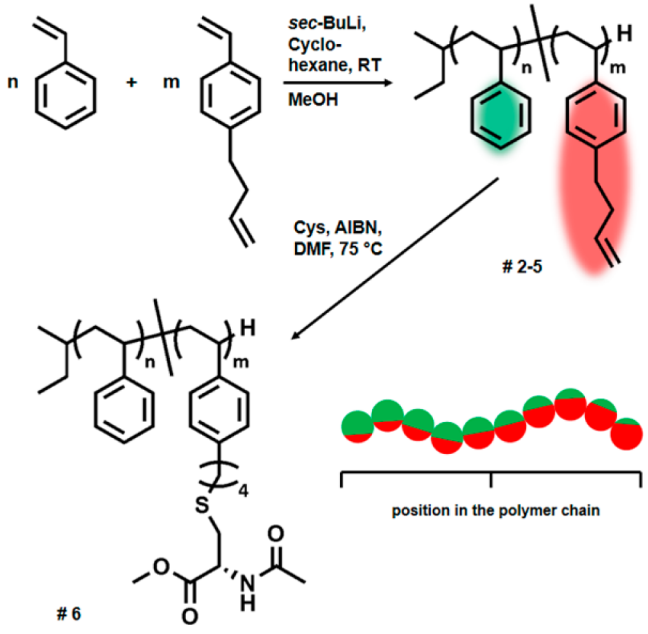

Also NMR spectra of the final copolymers allow determining the copolymer composition; however, for investigating the monomer sequence distribution within the copolymer chains, real-time ^{1}H NMR spectroscopy was employed. The carbanionic copolymerization was carried out in a conventional NMR tube in analogy to the batch procedure. The reaction mixture was prepared inside an argon-filled glovebox, and the tube was sealed with a rubber septum. Prior to the initiation of the polymerization, an ^{1}H NMR spectrum of the reaction mixture was recorded to calibrate the equipment and to determine the exact comonomer ratios in the comonomer mixture at t = 0 s (x(*p*BuS) = 0.55) by comparing the integrals of the styrenic vinyl double bonds of *p*BuS (δ = 5.58 ppm, dd, J = 15.4, 1.1 Hz and δ = 5.06 ppm, dd, J = 10.9, 1.1 Hz) and S (δ = 5.63 ppm, dd, J = 15.4, 1.1 Hz and δ = 5.11 ppm, dd, J = 10.9, 1.0 Hz). Subsequently, the reaction was initiated by the addition of *sec*-BuLi and the progress of the copolymerization monitored by real-time ^{1}H NMR spectroscopy over a period of 2.5 h. Every spectrum was recorded with four scans and a relaxation time of 1 s between the individual scans. The time between two measurements ranged from 0 to 42 s with increasing reaction time.

Figure 1 shows a selection of the ^{1}H NMR spectra measured during the copolymerization. With increasing time of the reaction the sharp signals of the monomers disappear, and simultaneously broad polymer resonances become more intense. In particular, the zoom-in clearly shows the decreasing intensity of the vinyl double bonds from both monomers (*p*BuS highlighted in red and S highlighted in green), indicating the consumption of the monomers and formation of the copolymer (note that the olefin resonances of the side chains (at 6.04–

dx.doi.org/10.1021/mz500255h | ACS Macro Lett. 2014, 3, 560−564

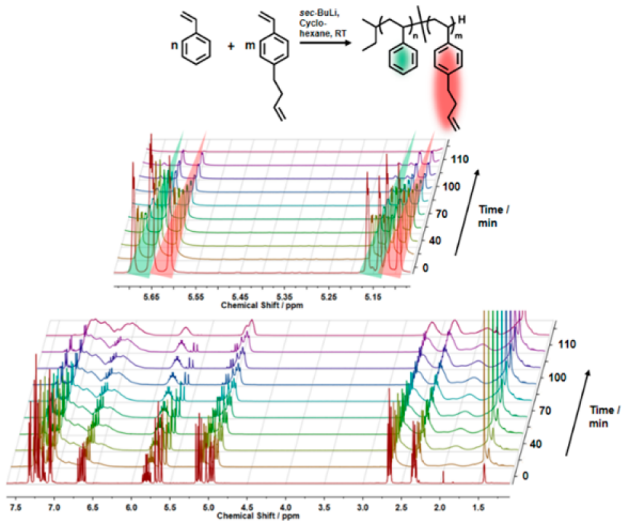

Figure 1. Real-time ^{1}H NMR copolymerization kinetics. Bottom: Overlay of spectra of the real-time ^{1}H NMR kinetics study. Top: Zoom-in, showing the consumption of *p*BuS (vinyl signals highlighted in red) and S (vinyl signals highlighted in green).

5.78 ppm and 5.20−4.88 ppm) remain unchanged after complete monomer consumption).

Figure 2a visualizes the normalized amount of unreacted monomer in stock vs the total conversion. From the measured values a fit curve was prepared. From these graphs it is clear that S (green) is incorporated into the copolymer faster than *p*BuS at the beginning of the polymerization, due to the lower electron density of the reactive vinyl double bond. Since in carbanionic polymerizations all polymer chains are initiated at the same time and there are no side reactions, the total conversion represents the average position of a single polymer chain. Thus, the probability of comonomer incorporation can be calculated for every point in the copolymer chains, which is visualized in Figure 2b. For an ideal random copolymerization the probability of incorporation for each monomer does not change during polymerization and therefore only depends on the initial concentration, resulting in a straight line in the diagram (dashed lines in Figure 2b). In the copolymer system, in the initial stages of the copolymerization the incorporation of S is preferred, although the molar ratio in stock is x(*p*BuS) = 0.55. Consequently with ongoing reaction time the concentration of S decreases. At 42% total conversion, equivalent to a mole fraction of x(*p*BuS) = 0.67 in stock, both monomers are incorporated equally (crossover point in Figure 2b). Figure 2c illustrates the results from Figure 2b schematically: each sphere represents 10% conversion, and the filling level represents the probability of the respective comonomer incorporation at this point.

Due to the different reactivity of both comonomers the relative monomer concentration in the stock changes steadily during the polymerization. Consequently the copolymerization, i.e., reactivity ratios, can also be determined by the classical Fineman−Ross formalism from the fitting curves (equation S1, SI).[31] Since the first measuring point was taken at 16% total conversion and the integrals of the monomers in stock above 80% total conversion become considerably small, we have taken the values in between into account to minimize the error of the calculated reactivity ratios. The results are shown in Figure 3. The slope of the straight line corresponds to r_1 = 3.07, indicating a preferred homopolymerization of S versus cross

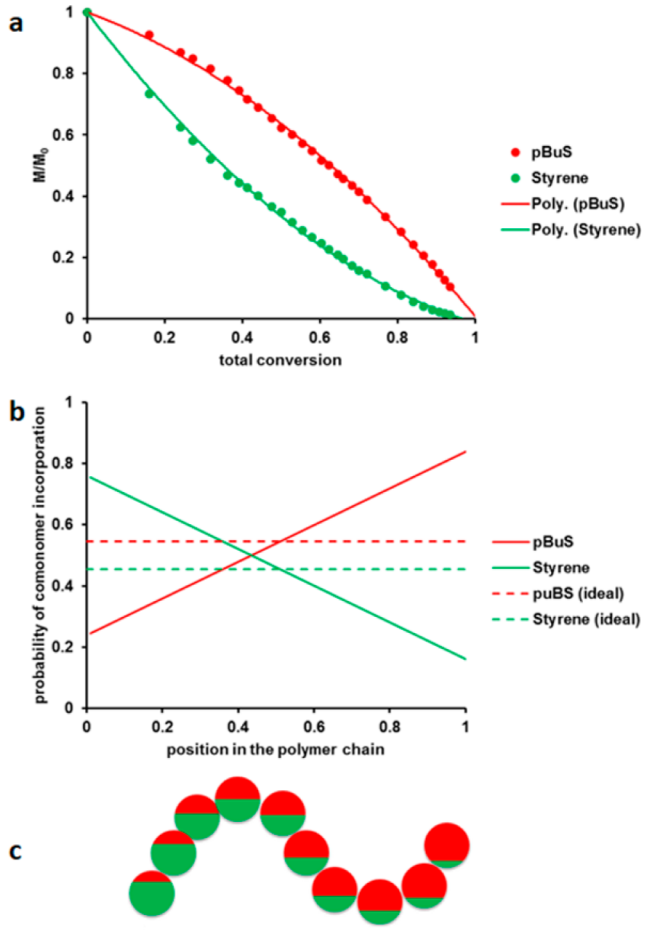

Figure 2. (a) Normalized monomer concentrations in the reaction mixture vs total conversion, (b) probability of comonomer incorporation vs relative position in the polymer chains (straight line) and theoretical incorporation in the case of an ideal random copolymerization (dashed line), and (c) corresponding visualization of the polymer chain for the P*p*BuS-*co*-PS copolymers.

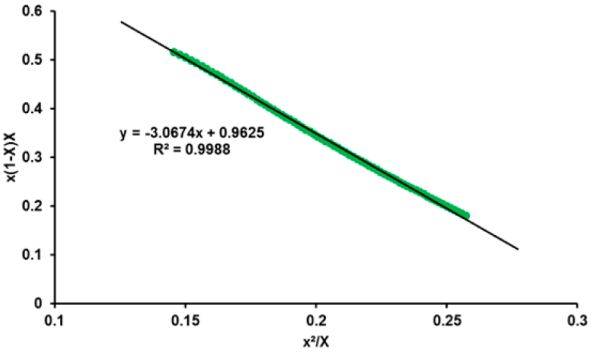

Figure 3. Determination of the reactivity ratios by the Fineman−Ross formalism for the system S/*p*BuS in cyclohexane at 23 °C. Counterion: lithium.

propagation (equation S2, SI). The *y*-axis section represents r_2 having a value of 0.96, which describes an almost equal ratio of homopolymerization of *p*BuS versus cross propagation.

Functional copolymers are useful for many potential fields of application. The average functional group distance is a relevant parameter for the postpolymerization functionalization to generate tailored structures, e.g., by the introduction of polar groups, labels, dyes, etc.[32] The polyvalent P*p*BuS-*co*-PS

dx.doi.org/10.1021/mz500255h | *ACS Macro Lett.* 2014, 3, 560−564

copolymers exhibit a gradient profile of the pendant double bonds which has to be taken into account for postfunctionalization. As a model reaction, we used the thiol−ene reaction with a protected cysteine derivative (Cys) to demonstrate the formation of conjugates. The reaction was initiated with azobis(isobutyronitrile) (AIBN) in dimethylformamide (DMF) at 75 °C. After work-up the resonances of the butenyl double bonds at 5.89 and 5.01 ppm have disappeared, and the corresponding signals of Cys appear at 8.39 and 4.48 ppm (Figure 4 displays the ^{1}H NMR spectra prior to (#4) and after (#6) functionalization), indicating quantitative functionalization.

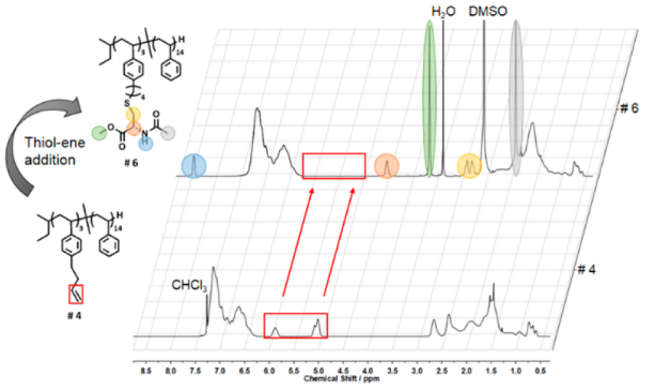

Figure 4. ^{1}H NMR spectra of the functionalization of PS_{14}-*co*-P*p*BuS_3 (#4) by the radical thiol−ene reaction PS_{14}-*co*-(P*p*BuS-Cys)$_3$ (#6).

In summary, we have investigated the synthesis of polyvalent P*p*BuS-*co*-PS with different molar fractions x(S) = 0−0.84 by LAP in cyclohexane at room temperature. The focus of this study was the determination of the functional group distribution. By limitation of the reaction time to 2.5 h, side reactions were suppressed, and copolymers with a narrow molecular weight distribution were obtained. A detailed understanding of the copolymerization behavior was achieved by real-time ^{1}H NMR spectroscopy. Due to the chemical similarity, classical methods such as the study of triad abundances cannot be employed for styrene and styrene derivatives to determine the comonomer distribution in detail. By real-time ^{1}H NMR spectroscopy the monomer content can be distinguished at every point of the copolymerization. Since in living anionic polymerizations all polymer chains are initiated at the same time, the probability of comonomer incorporation can be determined at every point of the copolymerization synonymously with every position of the polymer chain (Figure 2c). The chemically different monomers *p*BuS and S lead to a gradient polymer structure where S is incorporated preferably. Finally, we demonstrate the addressability of the butenyl double bonds of *p*BuS in the PS-*co*-P*p*BuS copolymer by performing a thiol−ene reaction with protected Cys. Further postmodifications such as hydrosilylation,[29] Diels−Alder, or cross-linking reactions demonstrate the versatile opportunities of this copolymer.

■ ASSOCIATED CONTENT

Ⓢ Supporting Information

Detailed experimental procedures as well as analytical and spectral characterization data. This material is available free of charge via the Internet at http://pubs.acs.org.

■ AUTHOR INFORMATION

Corresponding Authors

*E-mail: wurm@mpip-mainz.mpg.de (F.R.W.)
*E-mail: hfrey@uni-mainz.de (H.F.).

Notes

The authors declare no competing financial interest.

■ ACKNOWLEDGMENTS

A.N. thanks the Graduate School of Excellence MAINZ for financial support. F.R.W. thanks the Max Planck Graduate Center (MPGC) for support. We thank Prof. Axel H. E. Müller (JGU Mainz) and Markus Pauly (JGU Mainz) for valuable discussions as well as Kevin Tritschler for technical assistance.

■ REFERENCES

(1) Szwarc, M. *Nature* **1956**, *178*, 1168−1169.
(2) Hirao, A.; Goseki, R.; Ishizone, T. *Macromolecules* **2014**, *47*, 1883−1905.
(3) Baskaran, D.; Müller, Axel H. E. *Prog. Polym. Sci.* **2007**, *32*, 173−219.
(4) Quirk, R. P.; Hsieh, H. L. In *Anionic Polymerization: Principles And Practical Applications*; Hudgin, D. E., Ed.; Marcel Dekker Inc: New York, 1996; pp 261−306.
(5) Ito, S.; Goseki, R.; Ishizone, T.; Senda, S.; Hirao, A. *Macromolecules* **2013**, *46*, 819−827.
(6) Natalello, A.; Alkan, A.; Friedel, A.; Lieberwirth, I.; Frey, H.; Wurm, F. R. *ACS Macro Lett.* **2013**, *2*, 313−316.
(7) Carlotti, S.; Desbois, P.; Warzelhan, V.; Deffieux, A. *Polymer* **2009**, *50*, 3057−3067.
(8) Lutz, J.-F.; Ouchi, M.; Liu, D. R.; Sawamoto, M. *Science* **2013**, *341*, 1238149.
(9) Lutz, J.-F. *Acc. Chem. Res.* **2013**, *46*, 2696−2705.
(10) Ouchi, M.; Badi, N.; Lutz, J.-F.; Sawamoto, M. *Nat. Chem.* **2011**, *3*, 917−924.
(11) Brown, J. R.; Sides, S. W.; Hall, L. M. *ACS Macro Lett.* **2013**, 1105−1109.
(12) Yuki, H.; Hotta, J.; Okamoto, Y.; Murahashi, S. *Bull. Chem. Soc. Jpn.* **1967**, *40*, 2659−2663.
(13) Yuki, H.; Okamoto, Y. *Bull. Chem. Soc. Jpn.* **1969**, *42*, 1644−1649.
(14) Yuki, H.; Okamoto, Y. *Bull. Chem. Soc. Jpn.* **1970**, *43*, 148−151.
(15) Natalello, A.; Hall, J. N.; Eccles, E.; Alex, L.; Kimani, S. M.; Hutchings, L. R. *Macromol. Rapid Commun.* **2011**, *32*, 233−237.
(16) Brooks, P. P.; Natalello, A.; Hall, J. N.; Eccles, E.; Alex, L.; Kimani, S. M.; Bley, K.; Hutchings, L. R. *Macromol. Symp.* **2013**, *323*, 42−50.
(17) Obermeier, B.; Wurm, F.; Frey, H. *Macromolecules* **2010**, *43*, 2244−2251.
(18) Alkan, A.; Natalello, A.; Wagner, M.; Frey, H.; Wurm, F. R. *Macromolecules* **2014**, *47*, 2242−2249.
(19) Mangold, C.; Wurm, F.; Frey, H. *Polym. Chem.* **2012**, *3*, 1714−1721.
(20) Reuss, V. S.; Obermeier, B.; Dingels, C.; Frey, H. *Macromolecules* **2012**, *45*, 4581−4589.
(21) Tonhauser, C.; Alkan, A.; Schömer, M.; Dingels, C.; Ritz, S.; Mailänder, V.; Frey, H.; Wurm, F. R. *Macromolecules* **2013**, *46*, 647−655.
(22) Natalello, A.; Werre, M.; Alkan, A.; Frey, H. *Macromolecules* **2013**, *46*, 8467−8471.
(23) Williamson, D. T.; Buchanan, T. D.; Elkins, C. L.; Long, T. E. *Macromolecules* **2004**, *37*, 4505−4511.
(24) Storey, R. F.; Donnalley, A. B.; Maggio, T. L. *Macromolecules* **1998**, *31*, 1523−1526.
(25) Michel, A. J.; Puskas, J. E.; Brister, L. B. *Macromolecules* **2000**, *33*, 3518−3524.
(26) Long, T. E.; Liu, H. Y.; Schell, B. A.; Teegarden, D. M.; Uerz, D. S. *Macromolecules* **1993**, *26*, 6237−6242.

(27) Quinebèche, S.; Navarro, C.; Gnanou, Y.; Fontanille, M. *Polymer* **2009**, *50*, 1351−1357.
(28) Zhang, H.; Ruckenstein, E. *Macromolecules* **1999**, *32*, 5495−5500.
(29) Ruckenstein, E.; Zhang, H. *Macromolecules* **1999**, *32*, 6082−6087.
(30) Claudy, P.; Létoffé, J. M.; Camberlain, Y.; Pascault, J. P. *Polym. Bull.* **1983**, *9*−*9*, 208−215.
(31) Fineman, M.; Ross, S. D. *J. Polym. Sci.* **1950**, *5*, 259−262.
(32) Gauthier, M. A.; Gibson, M. I.; Klok, H.-A. *Angew. Chem., Int. Ed.* **2009**, *48*, 48−58.